

Patterns formed by paramagnetic particles in a horizontal layer of a magnetorheological fluid subjected to a dc magnetic field

 Tomofumi Ukai¹ and Toru Maekawa^{2,*}
¹REDS Group, Saitama Small Enterprise Promotion Corporation, SKIP City, Kawaguchi, Saitama 333-0844, Japan

²Bio-Nano Electronics Research Center, Toyo University, 2100, Kujirai, Kawagoe, Saitama 350-8585, Japan

(Received 27 May 2003; revised manuscript received 5 January 2004; published 31 March 2004)

We investigate the patterns formed by paramagnetic particles, which are dispersed in a liquid solvent subjected to a dc magnetic field. We calculate the dynamics of paramagnetic particles by the Brownian dynamics method based on the Langevin equation. We, in particular, focus on the effect of the system height on the pattern formations. We also discuss the mechanism of the pattern formations and the dynamics of the structure creation processes.

DOI: 10.1103/PhysRevE.69.032501

PACS number(s): 83.80.Gv, 61.90.+d

Magnetorheological (MR) fluids are usually composed of paramagnetic particles of 0.1–10 μm in diameter, which are dispersed in a solvent such as water or oil [1]. A magnetic dipole moment is induced in a paramagnetic particle when the particle is subjected to an external dc magnetic field, and therefore anisotropic interactions are induced among paramagnetic particles via the dipole-dipole potentials. When the dipole-dipole interactions are strong compared to thermal energy, particles form chain clusters in parallel to an external magnetic field [2–4]. Furthermore, secondary structures are created by the chain clusters through the chain-chain interactions [5–9]. The secondary structures may be changed dramatically depending on the volume fraction of colloidal particles, the number of particles in chain clusters (the cluster length), and the intensity of external magnetic fields (the intensity of the induced magnetic dipole moment). However, the effect of the system height on the creation of different structures has not yet been quantitatively investigated in either MR or electrorheological (ER) systems. The only cases to have been studied so far are those featuring relatively thick layers [10–16]. What is more, the actual mechanism and dynamics, through which different structures are created, have not yet been completely understood. In this Brief Report, we carry out Brownian dynamics analysis of an MR fluid system and investigate the patterns formed by paramagnetic particles. We focus, in particular, on the effect of the system height in the direction of an external dc magnetic field on the creation of structures in an MR fluid system.

Here, we introduce a numerical model of an MR fluid, which is confined between two parallel plates (see Fig. 1). Spherical paramagnetic particles are dispersed in a solvent and a dc magnetic field is applied perpendicular to the fluid layer. A magnetic dipole moment is induced in each particle in the direction of the external magnetic field as shown in Fig. 2. The interparticle potentials are the dipole-dipole potential u_d and a repulsive potential u_c through which particles cannot penetrate each other [7,9]. We also take into account a repulsive potential between a particle and the plates u_w [7,9]:

$$u_d = \frac{1}{4\pi\mu} \left\{ \frac{\mathbf{m}_i \cdot \mathbf{m}_j}{r_{ij}^3} - \frac{3}{r_{ij}^5} (\mathbf{m}_i \cdot \mathbf{r}_{ij})(\mathbf{m}_j \cdot \mathbf{r}_{ij}) \right\}, \quad (1)$$

$$u_c = \frac{|\mathbf{m}|^2}{4\pi\mu d^3} \exp\left\{-40\left(\frac{r_{ij}}{d}-1\right)\right\}, \quad (2)$$

$$u_w = \frac{|\mathbf{m}|^2}{4\pi\mu d^3} \exp\left\{-40\left(2\frac{w_i}{d}-1\right)\right\}, \quad (3)$$

where \mathbf{m}_i , μ , \mathbf{r}_{ij} , d , and w_i are, respectively, the magnetic dipole moment of particle i , the magnetic permeability, the displacement vector from particle j to particle i , the diameter of a particle, and the distance between particle i and a plate. In the present case, the distance σ corresponding to the minimum point of the interparticle potentials $u_d + u_c$, is $\sigma = 1.0525d$. The control parameters are the nondimensional system height $L \equiv L_z/d$ and the ratio of the dipole moment energy to thermal energy $\lambda \equiv |\mathbf{m}|^2/4\pi\mu d^3 kT$, where the system height L_z is nondimensionalized by d , and k and T are, respectively, the Boltzmann constant and the system tem-

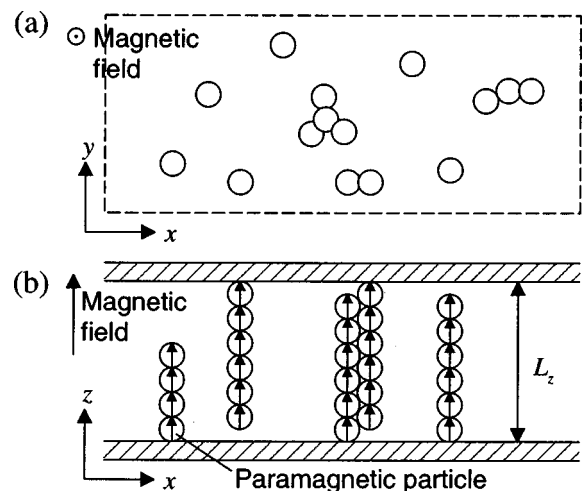


FIG. 1. Physical situations. (a) Top view, (b) side view. Paramagnetic particles are dispersed in a solvent. A dc magnetic field is applied in the z direction perpendicular to the fluid layer.

*Email addresses: trmkw@eng.toyo.ac.jp;
toru.maekawa@physics.org

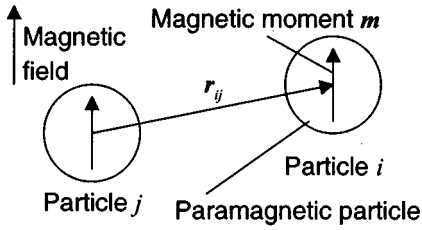


FIG. 2. Paramagnetic particles. A magnetic dipole moment is induced in the direction of an external magnetic field.

perature. We calculate the translational motions of the particles based on the Langevin equation

$$\mathbf{u} = (\mathbf{F} + m\mathbf{P})/\zeta, \quad (4)$$

where the inertial term is omitted supposing that the Stokes viscous resistance is predominant over the particles' ballistic movement, which is correct when the parameter $A \equiv mkT/(\zeta d)^2$ satisfies the following condition: $A \ll 1$ [17]. In the present case, $A \sim 10^{-7}$ (see the physical conditions explained below). \mathbf{u} , \mathbf{F} , and m are the velocity of a particle, the force acting on the particle and the mass of the particle. ζ is the friction coefficient between a particle and the solvent, which follows Stokes law; that is, $\zeta \equiv 3\pi\eta d$, where η is the dynamic viscosity of the solvent, and \mathbf{P} is random noise caused by the collisions of the solvent molecules with a particle [18]. We carried out calculations for $\lambda = 18$, $d = 0.2 \mu\text{m}$, ρ (mass density of a particle) $= 1382 \text{ kg/m}^3$, $\eta = 0.001 \text{ Pa s}$, $T = 300 \text{ K}$, $|\mathbf{m}| = 9.705 \times 10^{-23} \text{ Wb m}$, and $\mu = 4\pi \times 10^{-7} \text{ H/m}$, which are typical conditions for common MR fluids. Periodic boundary conditions were employed in the x and y directions (see Fig. 1). The dimensions of the calculation space in the x and y directions were $22.88 d \times 22.88 d$ in the case of $L \leq 11$ and $16.18 d \times 16.18 d$ in the case of $11 < L$. The number of particles were changed from 400 to 4000 depending on the system height. The particles were randomly placed initially. The volume fraction of particles ρ_V were changed from 0.05 to 0.4, but in this Brief Report, we focus on $\rho_V = 0.2$ since it is most interesting from the point of view of pattern formations. The iteration time interval was $0.1 \mu\text{s}$.

Now, we investigate the effect of the system height L on the patterns created by paramagnetic particles for $2.0 \leq L \leq 40$. First, we focus on the cases when the system height is very short ($L < 5$). The top views of the steady-state patterns formed by the paramagnetic particles are shown in Fig. 3, where the external uniform magnetic field is applied in a direction perpendicular to the horizontal plane. As is clearly seen, the patterns formed in the system are very sensitive to the system height; that is, individually dispersed chains [see Figs. 3(a) and 3(d)] and meandering walls [Figs. 3(c) and 3(f)] appear in turn cyclically with an increase in the system height. Basically, there is no branch along the walls. Under a certain height, walls and individual chains coexist [Figs. 3(b) and 3(e)]. Next, we focus on the cases when the system height is in the intermediate range ($5 \leq L < 12$). The top views of the steady-state patterns are shown in Figs. 4(a)–

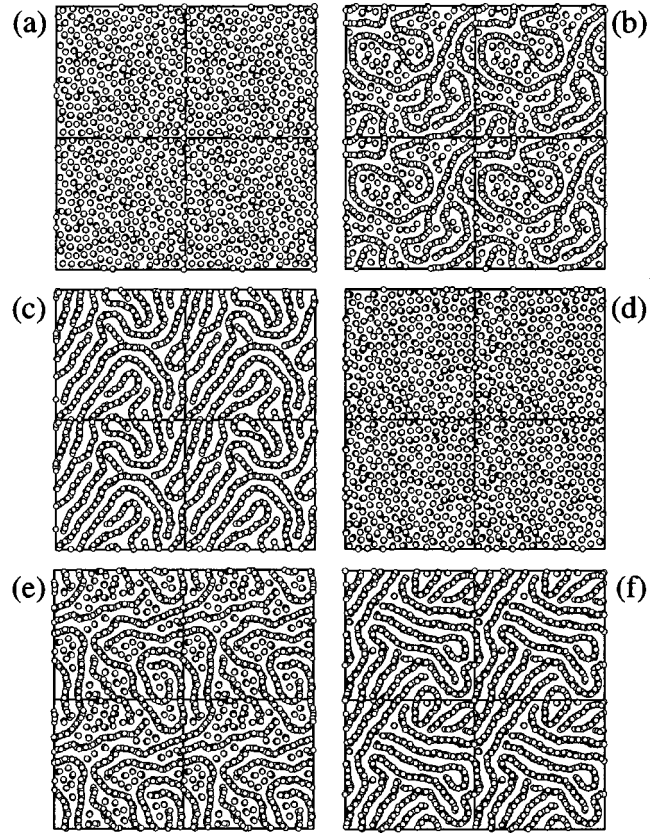


FIG. 3. Top views of cluster structures created by paramagnetic particles when the system height is short ($L < 5$). (a) $L = 3.4$, (b) $L = 3.6$, (c) $L = 3.8$, (d) $L = 4.4$, (e) $L = 4.6$, (f) $L = 4.8$.

4(c). The pattern formations are still sensitive to the system height; that is, individual chains [Fig. 4(a)], walls [Fig. 4(c)], and a mixture of chains and walls [Fig. 4(b)] appear cyclically with an increase in the system height. However, there are, in fact, gradual changes in the internal structures of the walls, which will be discussed in detail later. Once L exceeds 12, the pattern formations become different from those for $L < 12$. The top views of the patterns created when $L = 13$, 20, and 40 are shown in Figs. 4(d)–(f). When $12 \leq L \leq 40$, the above cyclic formations of chains and walls no longer appear. Walls such as those shown in Figs. 4(d)–(f) are always formed, instead. However, the internal structures of the walls are different from those created in the case of $L < 12$, which will also be discussed later. There are branches along these walls in contrast with the short system cases. As the system height increases, the walls become thicker [Figs. 4(e) and 4(f)] and body-centered-tetragonal (bct) structures are formed by the paramagnetic particles in the walls.

In order to overview the relation between the cluster structures and the system height, we define the connectivities C_{0° , C_{30° , and C_{60° as follows:

$$C_{0^\circ} \equiv \frac{C_{cp}(0^\circ \leq |\varphi| \leq 20^\circ)}{N},$$

$$C_{30^\circ} \equiv \frac{C_{cp}(20^\circ \leq |\varphi| \leq 40^\circ)}{N},$$

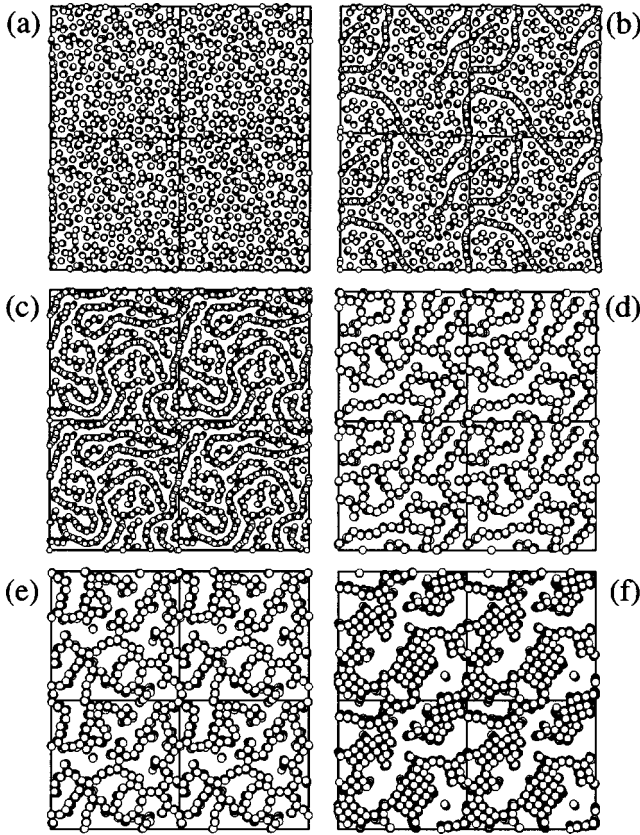


FIG. 4. Top views of cluster structures created by paramagnetic particles when the system height is greater than 5. (a) $L=7.4$, (b) $L=7.6$, (c) $L=7.8$, (d) $L=13$, (e) $L=20$, (f) $L=40$.

$$C_{60^\circ} \equiv \frac{C_{cp}(50^\circ \leq |\varphi| \leq 70^\circ)}{N}, \quad (5)$$

where C_{cp} is the number of particles contacting at angle, φ , which lies between the indicated values, and N is the total number of particles in the system. Therefore, C_{0° , C_{30° , and C_{60° represent the average number of particles contacting at angles 0° , 30° , and 60° , respectively. The dependence of the steady-state connectivities on the system height is shown in Fig. 5. Note that when C_{0° is large and both C_{30° and C_{60° are very small, chain clusters are dispersed individually in the system, whereas when C_{30° is large and both C_{0° and C_{60° are very small, wall A's, in which particles are located such as those shown in Fig. 6, are created in the system. When both C_{0° and C_{60° are large and C_{30° is small, on the other hand, wall B's are created in the system (see Fig. 6). When $L < 5$, C_{0° and C_{30° fluctuate with an increase in the system height, while C_{60° is almost zero. C_{0° becomes maximum at the system height, at which C_{30° becomes minimum, and vice versa. Therefore, individually dispersed chain clusters and wall A's appear in turn cyclically as the system height increases up to $L=5$. However, as the system height increases from $L=5$ to 12 , although the periodic features in C_{0° and C_{30° are still maintained, the local minimum values of C_{0° increase, the local maximum values of C_{30° decrease, and C_{60° increases fluctuatingly. The wall structures change gradually from wall A's to wall B's. Once L exceeds 12 , the

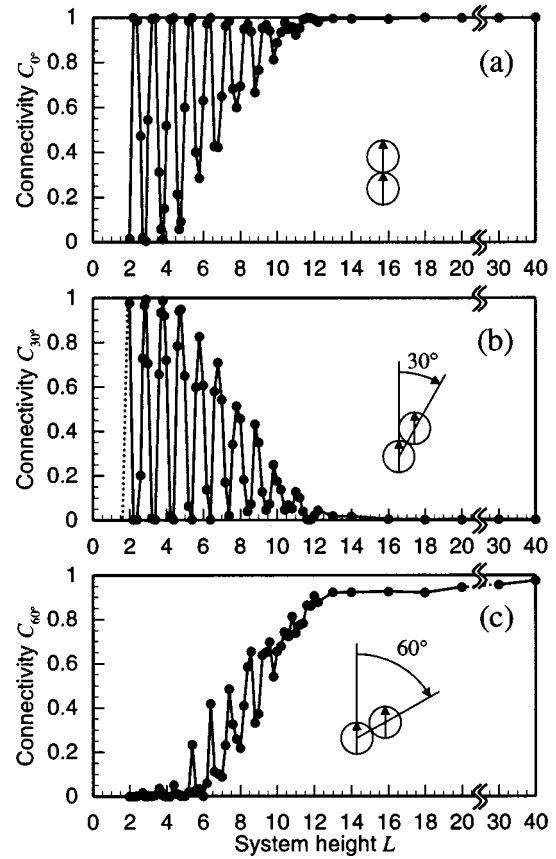


FIG. 5. Dependence of connectivities C_{0° , C_{30° , and C_{60° on the system height L . (a) C_{0° , (b) C_{30° , (c) C_{60° .

above cyclic features disappear and both C_{0° and C_{60° become large, while C_{30° is almost zero. In other words, wall B's are created in the system. We also analyzed the dynamic process of the pattern formations. When walls are created for $L < 5$, both C_{0° and C_{30° increase in the early stage, but C_{0° decreases quickly. This means that wall A's are formed from the beginning and chains quickly disintegrate. Wall A's are not created via chain-chain interactions. When walls are formed for $12 < L$, C_{0° increases very quickly and C_{60° increases gradually. In other words, straight chains are formed at first and they coagulate together to form wall B's. When the system is high, the time constant for the creation of

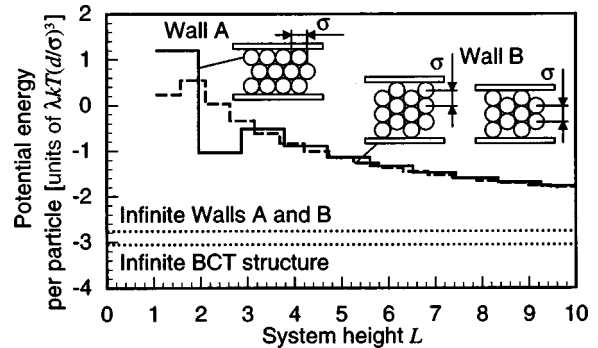


FIG. 6. Dependence of potential energy per particle of single walls on system height. —: single wall A; ---: single wall B.

chains is much shorter than that for the creation of walls. The secondary structures, that is, wall B 's, are created through chain-chain interactions, whereas when the system is low, as we mentioned, wall A 's are formed in the very early stages.

Chain clusters can be dispersed stably when the nondimensional system height L coincides with the cluster length. Repulsive forces act between two parallel chains in this case. Such stably dispersed chains were observed in MR and ER fluids in short system cases [7,10]. When the system height is short, although both wall A 's and wall B 's can be formed from a geometrical point of view, wall A 's are created rather than wall B 's since the internal potential energy of a single wall A is much lower than that of a single wall B (see Fig. 6, where, on the basis of the calculation carried out by Tao and Sun [10], we obtained the energies of a single wall A and a single wall B , which are extended infinitely in the horizontal direction, as a function of the wall height). As the number of particles increases, the difference in the potential energies between a single wall A and a single wall B becomes smaller and once L exceeds 12, there is no distinctive difference in the energies. Note that the energy per particle of a single wall A is equal to that of a single wall B ; $-2.7584\lambda kT(d/\sigma)^3$, when the walls are extended infinitely in both horizontal and vertical directions according to Sun and Tao [19]. Since chains are formed in the early stages and walls are created through chain-chain coagulations when L is greater than 12, wall B 's are created rather than wall A 's. Wall B 's were actually observed in MR systems [7,8] and ER systems [13,14]. However, when L is very large, since the length of chains cannot reach the system height, chains of different sizes coagulate to form columns, in which bct structures are created. Note that the internal energy of a bct column becomes lower than that of a wall B for the same number of particles as the number of particles increases. The energy per particle in an infinite bct column is $-3.0501\lambda kT(d/\sigma)^3$, which is lower than that of a single wall B [14,19]. bct col-

umns were observed in MR systems [8,9] and ER systems [11–14].

In summary, we investigated the pattern formations created by paramagnetic particles and clarified the effect of the system height on the pattern formations. Although a variety of structures have been reported through numerical and experimental studies on pattern formations in MR and ER systems, the physical conditions were not always the same. Therefore, in this Brief Report, we focused on the effect of the system height on the pattern formations, fixing the volume fraction of particles ρ_V at 0.2. When ρ_V is less than 0.2, only individually dispersed chains appear when the system is low and wall B 's are created as the system height increases. When ρ_V is greater than 0.3, solid-state domains appear in the system. We will discuss the pattern formations for $\rho_V \neq 0.2$ in detail on another occasion. We also fixed the value of the control parameter λ at 18. In this case, thermal energy is still low compared to the interactive energy. According to Morimoto and Maekawa [18], the interactive energy becomes predominant when $8 \leq \lambda$. However, the effect of λ on the pattern formation in finite MR fluid systems has not yet been investigated systematically [9]. The value of λ can, in general, vary from 0 to 10^3 even under the standard conditions [3,4,20]. Therefore, we will also be investigating the effect of λ on the cluster structures and formation processes in detail.

This study has been supported by a grant for the 21st Century's Center of Excellence Programs organized by the Ministry of Education, Culture, Sports, Science and Technology, Japan, since 2003, a grant for the Rational Evolutionary Design of Advanced Biomolecules Project organized by the Japan Science and Technology Agency (JST) since 2002, and The Asahi Research Fund for Natural Sciences organized by Asahi Glass Co. since 2001. T.U. would like to thank JST for financial support.

-
- [1] *Proceedings of the Eighth International Conference on Electrorheological Fluids and Magnetorheological Suspensions*, edited by G. Bossis (World Scientific, Singapore, 2002).
- [2] P. G. de Gennes and P. A. Pincus, *Phys. Kondens. Mater.* **11**, 189 (1970).
- [3] M. Fermiger and A. P. Gast, *J. Colloid Interface Sci.* **154**, 522 (1992).
- [4] J. H. E. Promislow, A. P. Gast, and M. Fermiger, *J. Chem. Phys.* **102**, 5492 (1995).
- [5] M. Gross and S. Kiskamp, *Phys. Rev. Lett.* **79**, 2566 (1997).
- [6] T. C. Halsey and W. Toor, *J. Stat. Phys.* **61**, 1257 (1990).
- [7] M. Mohebi, N. Jamasbi, and J. Liu, *Phys. Rev. E* **54**, 5407 (1996).
- [8] J. E. Martin, K. M. Hill, and C. P. Tigges, *Phys. Rev. E* **59**, 5676 (1999).
- [9] G. L. Gulley and R. Tao, *Int. J. Mod. Phys. B* **15**, 851 (2001).
- [10] R. Tao and J. M. Sun, *Phys. Rev. Lett.* **67**, 398 (1991).
- [11] T.-j. Chen, R. N. Zitter, and R. Tao, *Phys. Rev. Lett.* **68**, 2555 (1992).
- [12] G. L. Gulley and R. Tao, *Phys. Rev. E* **56**, 4328 (1997).
- [13] J. E. Martin, R. A. Anderson, and C. P. Tigges, *J. Chem. Phys.* **108**, 3765 (1998).
- [14] U. Dassanayake, S. Fraden, and A. van Blaaderen, *J. Chem. Phys.* **112**, 3851 (2000).
- [15] D. J. Kingenber, F. van Swol, and C. F. Zukoski, *J. Chem. Phys.* **91**, 7888 (1989).
- [16] J. M. Sun and R. Tao, *Phys. Rev. E* **53**, 3732 (1996).
- [17] H. X. Guo, Z. H. Mai, and H. H. Tian, *Phys. Rev. E* **53**, 3823 (1996).
- [18] H. Morimoto and T. Maekawa, *J. Phys. A* **33**, 247 (2000).
- [19] J. M. Sun and R. Tao, *Phys. Rev. E* **53**, 3732 (1996).
- [20] S. Cutillas and J. Liu, *Phys. Rev. E* **64**, 011506 (2001).